Geobiology

Geobiology (2012) DOI: 10.1111/j.1472-4669.2012.00320.x

Geobiological constraints on Earth system sensitivity to CO_2 during the Cretaceous and Cenozoic

D. L. ROYER,[1] M. PAGANI[2] AND D. J. BEERLING[3]

[1]*Department of Earth and Environmental Sciences and College of the Environment, Wesleyan University, Middletown, CT, USA*
[2]*Department of Geology and Geophysics, Yale University, New Haven, CT, USA*
[3]*Department of Animal and Plant Sciences, University of Sheffield, Sheffield, UK*

ABSTRACT

Earth system climate sensitivity (ESS) is the long-term (>10^3 year) response of global surface temperature to doubled CO_2 that integrates fast and slow climate feedbacks. ESS has energy policy implications because global temperatures are not expected to decline appreciably for at least 10^3 year, even if anthropogenic greenhouse gas emissions drop to zero. We report provisional ESS estimates of 3 °C or higher for some of the Cretaceous and Cenozoic based on paleo-reconstructions of CO_2 and temperature. These estimates are generally higher than climate sensitivities simulated from global climate models for the same ancient periods (approximately 3 °C). Climate models probably do not capture the full suite of positive climate feedbacks that amplify global temperatures during some globally warm periods, as well as other characteristic features of warm climates such as low meridional temperature gradients. These absent feedbacks may be related to clouds, trace greenhouse gases (GHGs), seasonal snow cover, and/or vegetation, especially in polar regions. Better characterization and quantification of these feedbacks is a priority given the current accumulation of atmospheric GHGs.

Received 27 July 2011; accepted 19 January 2012

Corresponding author: D. L. Royer. Tel.: +860 685 2836; fax: +860 685 3651; e-mail: droyer@wesleyan.edu

INTRODUCTION

Climate sensitivity (CS) is the equilibrium change in global mean near-surface air temperature for a doubling of atmospheric CO_2 above pre-industrial values (e.g., IPCC, 2007). In a simple blackbody system, this radiative forcing (3.7 W m^{-2}) causes an approximately 1.2 °C warming (e.g., Charney *et al.*, 1979; Soden & Held, 2006). However, feedbacks such as changes in atmospheric water vapor content and cloud distributions amplify or dampen the temperature effect associated with CO_2. CS can therefore be expressed as

$$\mathrm{CS} = \frac{1.2\,^{\circ}\mathrm{C}}{1-f} \quad (1)$$

where f is the net impact of feedback processes. In a landmark study based on global climate model (GCM) simulations, Charney *et al.* (1979) calculated a CS of 3 ± 1.5 °C (50% confidence interval), with feedbacks positively contributing to the temperature increase. This value, and its associated uncertainty (Roe & Baker, 2007; Knutti & Hegerl, 2008), has not significantly changed over the subsequent three decades of intense research using increasingly sophisticated climate models, historical records, and sedimentary archives dating to the Last Glacial Maximum. For example, the IPCC (2007) reports an expected CS of 3 °C with a 66% likelihood range of 2.0–4.5 °C.

The goal of the present study is to place some first-order constraints on CS for the Cretaceous and Cenozoic using proxy evidence of CO_2 and temperature. Because of the temporal coarseness of the geologic record, our estimates represent a modified version of CS called Earth system sensitivity, described next. Given the uncertainties in our analysis, including considerable scatter in the CO_2 and temperature data, we aim not to calculate a best-fit estimate of CS, but rather to gauge whether there is reasonable evidence for CS exceeding 3 °C during at least part of the studied interval. As proxy reconstructions continue to improve and a clearer view of ancient CO_2 and temperature emerges, more robust assessments of CS will be possible.

Earth system climate sensitivity (ESS)

The primary climate feedbacks considered by Charney *et al.* (1979) and implemented in the majority of GCMs – changes

in atmospheric water vapor content and cloud, snow, and sea ice distributions – all operate on relatively short timescales (<10 year). Some GCMs also include effects related to aerosols, vegetation, and other greenhouse gases (GHGs) (IPCC, 2007). For simplicity, we use the term 'Charney sensitivity' to describe the 'fast-feedback' CS calculated by all of these models. Some climate feedbacks excluded from the concept of Charney sensitivity, such as the waxing and waning of continental ice sheets, impact climate primarily on longer timescales (>10^2 year). During globally warm times characterized by little-to-no permanent ice, potentially important 'fast-feedback' effects are excluded from Charney sensitivity too, for example, the behavior of clouds (Kump & Pollard, 2008) and the mixing ratios of other trace GHGs (e.g., CH_4, N_2O) (Beerling *et al.*, 2011).

A calculation of CS that includes fast- and slow-feedbacks has been termed ESS (Hansen *et al.*, 2008; Lunt *et al.*, 2010) and can be formalized as

$$\mathrm{ESS} = \frac{1.2\,^{\circ}\mathrm{C}}{1 - (f_{\mathrm{C}} + f_{\mathrm{NC}})} \qquad (2)$$

where f_C reflects Charney feedbacks and f_{NC} all other feedbacks. The ESS concept has been defined in a variety of ways. For example, the modeling study of Lunt *et al.* (2010) includes feedbacks associated with vegetation and ice sheets, but other factors are either prescribed as external forcings (e.g., non-CO_2 GHGs) or not considered at all (e.g., some atmospheric chemistry reactions; Beerling *et al.*, 2011). In contrast, a proxy-based approach for estimating ESS, which typically involves estimates of CO_2 and temperature (e.g., Pagani *et al.*, 2010), embodies the full spectrum of climate forcings and feedbacks at the associated temporal resolution of the proxy data. In other words, no climate component is missing. However, a tacit assumption for components that cannot be reconstructed is that they covary with the climate state (i.e., that they are climate feedbacks, not external forcings). If this assumption is incorrect, for example if methane concentrations do not covary strongly with the climate state, then uncertainty in the ESS estimates increases.

Earth system climate sensitivity is more relevant than Charney sensitivity for understanding the ancient past because of the limits in temporal resolution of many geologic archives (often >10^3 year) and because Charney sensitivity excludes some climate feedbacks important in Earth's past. ESS also has relevance to the present-day by providing insights into the possible spectrum of long-term responses of the Earth system to anthropogenic atmospheric CO_2 increase. Although the full extent of future warming associated with ESS will likely develop over centuries to millennia, it potentially contributes to important temperature effects on shorter timescales. For example, some processes absent in Charney sensitivity respond on decadal timescales, including melting of continental ice sheets (Chen *et al.*, 2006) and poleward migration of tree lines (Sturm *et al.*, 2001; Lloyd, 2005). Moreover, it is now recognized that global temperatures will not cool appreciably for many centuries, even if anthropogenic greenhouse gas emissions drop to zero (Archer & Brovkin, 2008; Matthews & Caldeira, 2008; Shaffer *et al.*, 2009; Solomon *et al.*, 2009, 2010; Armour & Roe, 2011; Friedlingstein *et al.*, 2011; Gillett *et al.*, 2011). This is primarily because the transfer of heat and diffusion of CO_2 to the ocean are both linked to ocean circulation (e.g., Solomon *et al.*, 2009). Critically, these projections of near-constant temperature are based on climate models with a Charney-style CS, even though their temporal scope overlaps with ESS. In this regard, estimations of ESS highlight the potential longer-term consequences of delaying policies for curbing greenhouse gas emissions (Archer, 2005; Montenegro *et al.*, 2007).

Prior estimates of Earth system climate sensitivity

The early Pliocene (5-3 million years ago, Ma) has received considerable attention because of the high density of paleoclimate information and because it may serve as a useful analog for the near future. At peak Pliocene warmth 4–5 Ma, global surface temperatures were approximately 4 °C warmer than pre-industrial conditions (Brierley & Fedorov, 2010). Coeval CO_2 estimates from a variety of approaches all indicate approximately 400 ppm, or approximately 0.5 CO_2 doublings relative to the pre-industrial (van der Burgh *et al.*, 1993; Raymo *et al.*, 1996; Pagani *et al.*, 2010; Seki *et al.*, 2010). After consideration of the uncertainties in the CO_2 and temperature estimates, a minimum ESS of 6 °C is implicated (Table 1) compared to a GCM-derived Charney sensitivity of 3 °C (Lunt *et al.*, 2010). Paleoclimate analyses for the Pleistocene and Cenozoic glacial period (last 34 million years) also indicate an approximately 6 °C ESS (Hansen *et al.*, 2008). The twofold amplification of ESS over Charney sensitivity is probably driven mostly by cryogenic feedbacks related to continental ice sheets (Hansen *et al.*, 2008; Pagani *et al.*, 2010).

The apparent importance of cryogenic feedbacks raises the fundamental question of the nature of ESS during times in Earth's history lacking large ice sheets. The early Cretaceous to early Cenozoic (125-34 Ma) is key for addressing this question because it is the most recent and data-rich greenhouse interval (Table 1) (Frakes *et al.*, 1992; Royer, 2006; Vaughan, 2007). Over the past 10 years, many temperature reconstructions for this interval have warmed (Huber, 2008) while some CO_2 estimates have dropped (Breecker *et al.*, 2010), implying an upward revision in ESS (Royer, 2010; Kiehl, 2011) and rendering earlier attempts at constraining ESS outdated (Budyko *et al.*, 1987; Hoffert & Covey, 1992; Covey *et al.*, 1996; Borzenkova, 2003) (Table 1).

Earth system climate sensitivity during the Paleocene–Eocene thermal maximum (PETM) approximately 55 Ma probably exceeded 3 °C (Higgins & Schrag, 2006; Pagani *et al.*, 2006; Zeebe *et al.*, 2009). The PETM may be a partial

Table 1 Published proxy-based estimates of Earth system climate sensitivity (ESS)

Time period	ESS (°C)	Reference
Large ice sheets present		
Pleistocene (last 400 000 year)	6	Hansen *et al.* (2008)
Pliocene (5-3 Ma)	>7	Pagani *et al.* (2010)
Pliocene (5-3 Ma)	6*	Budyko *et al.* (1987) and Borzenkova (2003)
Cenozoic glacial (34-0 Ma)	6	Hansen *et al.* (2008)
Phanerozoic glacial (340-260, 40-0 Ma)	>6	Park & Royer (2011)
Large ice sheets absent		
Late Eocene (35 Ma)	High	Kiehl (2011)
MECO (40 Ma)	2–5	Bijl *et al.* (2010)
Early Eocene (55 Ma)	2.4*,†	Covey *et al.* (1996)
PETM (55.5 Ma)	4	Higgins & Schrag (2006)
PETM (55.5 Ma)	High	Pagani *et al.* (2006)
PETM (55.5 Ma)	High	Zeebe *et al.* (2009)
Cretaceous (100 Ma)	3.4*,†	Hoffert & Covey (1992)
Cretaceous-early Paleogene (110-45 Ma)	3.7*	Budyko *et al.* (1987) and Borzenkova (2003)
Phanerozoic non-glacial (420-340, 260-40 Ma)	>3	Park & Royer (2011)

PETM, Paleocene–Eocene thermal maximum; MECO, Middle Eocene climatic optimum; Ma, million years ago.
All values are approximate. Park & Royer (2011) updates Royer *et al.* (2007).
*Recalculated treating changes in albedo as a feedback, not a forcing.
†Recalculated assuming 3.7 W m^{-2} for the radiative forcing of doubled CO_2 (IPCC, 2007).

analog of present-day climate change in terms of rate and magnitude of carbon release (Zachos *et al.*, 2008), albeit in an ice-free world. Bijl *et al.* (2010) produced a CO_2 and temperature record for the Middle Eocene climatic optimum (MECO; 40 Ma) and calculated an ESS of 2–5 °C (Table 1). In a study encompassing most of the Phanerozoic, Park & Royer (2011) optimized the value of ESS embedded in a long-term carbon cycle model to minimize the misfit in atmospheric CO_2 between the model and proxies. The most probable ESS values exceeded 3 °C during non-glacial intervals and 6+ °C during glacial periods (Table 1), although the time resolution was coarse (10 million-year time-steps).

Elevated ESS relative to Charney sensitivity is observed for some glacial times but far less is known for non-glacial times outside of a few brief intervals (e.g., PETM, MECO). Here, we aim to place better constraints on ESS during these warm times to evaluate the role of non-Charney feedbacks. Our primary goal is to test the strength of evidence for ESS exceeding Charney sensitivity and to discuss the climate feedbacks that may be responsible for any amplification.

METHODS

We compiled temperature records for the last 125 million years from literature sources (Table 2). We use the Zachos *et al.* (2008) and Cramer *et al.* (2009) compilations of benthic foraminifera $\delta^{18}O$ corrected for vital effects (Zachos *et al.*, 2001) as a proxy for deep-water temperature. We also compiled tropical sea surface temperature (SST) data from three methods: $\delta^{18}O$ of planktonic foraminifera, Mg/Ca of planktonic foraminifera, and TEX_{86} of archaeal membrane lipids. All $\delta^{18}O$ records were chosen carefully to avoid diagenetically altered material (Pearson *et al.*, 2001; Huber, 2008). We convert TEX_{86} data to SST using the (sub)tropical TEX_{86}^{H} calibration of Kim *et al.* (2008). For tropical $\delta^{18}O$ records, errors follow Crowley & Zachos (2000) (1 standard deviation = ±2.8 °C), who summarized uncertainties related to analytical error, $\delta^{18}O$-SST calibration, metabolism, depth habitat, and regional climate variability. For TEX_{86} records, we adopt the calibration standard error calculated by Kim *et al.* (2008) (±2.5 °C). For Mg/Ca records, errors are based on the likely range of marine Mg/Ca values discussed in the individual publications.

We compiled proxy CO_2 records from the stomatal, phytoplankton, boron, B/Ca, liverwort, and nahcolite methods (Table 2). All liverwort-based estimates are updated using the atmospheric $\delta^{13}C$ record of Tipple *et al.* (2010). We exclude

Table 2 CO_2 and temperature records used in study

Climate record	References
CO_2-stomata	Kürschner *et al.* (1996, 2001, 2008), McElwain (1998), Royer *et al.* (2001b), Beerling *et al.* (2002, 2009b), Greenwood *et al.* (2003), Royer (2003), Haworth *et al.* (2005), Passalia (2009), Retallack (2009), Quan *et al.* (2010), Smith *et al.* (2010) and Doria *et al.* (2011)
CO_2-phytoplankton	Pagani *et al.* (2005b, 2011) and Seki *et al.* (2010)
CO_2-boron	Pearson *et al.* (2008) and Seki *et al.* (2010)
CO_2-B/Ca	Tripati *et al.* (2009)
CO_2-liverworts	Fletcher *et al.* (2008)
CO_2-nahcolite	Lowenstein & Demicco (2006)
Temp-tropical $\delta^{18}O$	Wilson & Opdyke (1996), Pearson *et al.* (2001, 2007), Wilson & Norris (2001), Norris *et al.* (2002), Wilson *et al.* (2002), Moriya *et al.* (2007), Pucéat *et al.* (2007) and Bornemann *et al.* (2008)
Temp-tropical Mg/Ca	Tripati *et al.* (2003), Bice *et al.* (2006) and Sexton *et al.* (2006)
Temp-tropical TEX_{86}	Schouten *et al.* (2003), Dumitrescu *et al.* (2006), Forster *et al.* (2007a,b), Pearson *et al.* (2007) and Wagner *et al.* (2008)
Temp-benthic $\delta^{18}O$	Cramer *et al.* (2009) and Zachos *et al.* (2008)

paleosol calcite- and goethite-based CO_2 estimates because of uncertainties in modeling soil respiration (Breecker *et al.*, 2009) and isotopic fractionation factors (Rustad & Zarzycki, 2008), respectively. Boron-based CO_2 estimates of Pearson & Palmer (2000) are excluded because of problems related to diagenesis, vital effects of extinct species, and the evolution of seawater $\delta^{11}B$ and alkalinity (Lemarchand *et al.*, 2000; Royer *et al.*, 2001a; Pagani *et al.*, 2005a; Klochko *et al.*, 2006, 2009). Proxy-based CO_2 estimates have asymmetric probability distributions and are less bounded at high CO_2 (Royer *et al.*, 2001a) except for nahcolite-based estimates, which have a flat probability (equal likelihood) between 1125 and 2985 ppm. The errors plotted in Fig. 1A represent the standard error of the calibration function for the stomatal proxy, a variety of environmental, physiological, and calibration uncertainties for the phytoplankton and liverwort proxies, and mineral phase relationships for the nahcolite proxy; the nahcolite estimates will likely be revised downward following new mineral equilibria experiments (Jagniecki *et al.*, 2010).

Compiled atmospheric CO_2 and temperature records show scatter at any given time slice (Fig. 1A–C); CO_2, for example, typically varies up to twofold (Beerling & Royer, 2011). Given these uncertainties, and given that the probability distribution of CS is asymmetric and much more sharply defined at the lower boundary (IPCC, 2007; Roe and Armour, 2011), for most analyses we conservatively calculate ESS based on maximum estimates of atmospheric CO_2 and minimum estimates of global mean surface temperature. This approach establishes the likely minimum level of long-term warming for any CO_2 change.

Calculation of Earth system climate sensitivity: 125-45 Ma

We present two discrete analyses of ESS. The first focuses on the largely ice-free 125-45 Ma interval. We calculate changes in global annual-mean surface temperature relative to pre-industrial conditions following two approaches (Hansen *et al.*, 2008). First, tropical SSTs are converted to global mean surface temperature assuming a 2:3 scaling, consistent with Pleistocene records (Hansen *et al.*, 2008), and a pre-industrial tropical SST of 29 °C (Fig 1B). We note that our pre-industrial baseline is warm (compare with blue band in Fig. 1B) and that the 2:3 scaling is likely too conservative because latitudinal temperature gradients during the Cretaceous and early Paleogene were flatter than the present-day (Greenwood & Wing, 1995; Bice & Norris, 2002; Bijl *et al.*, 2009; Hollis *et al.*, 2009). A cooler SST baseline and a larger scaling factor both increase the calculation of global mean surface temperature and ESS. For example, during the Middle Eocene (approximately 40 Ma), a period of flatter-than-present latitudinal temperature gradients (Bijl *et al.*, 2009), Kiehl (2011) used tropical and subpolar SST records (35–40 and 20–25 °C, respectively) to calculate a global temperature approximately 16 °C warmer than pre-industrial

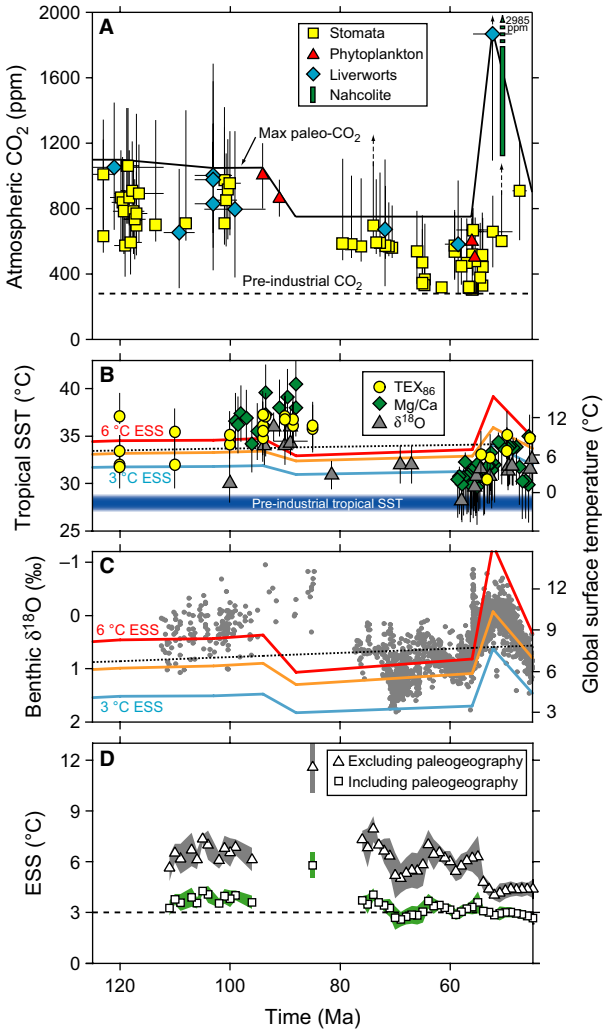

Fig. 1 Atmospheric CO_2, temperature, and Earth system climate sensitivity (ESS) during the Cretaceous and early Paleogene. (A) Atmospheric CO_2 from multiple proxy approaches. Estimates with unbounded upper limits are noted with arrows. The max paleo-CO_2 line is determined from the highest estimates at any given time. (B) Tropical sea surface temperature (SST) and (C) benthic $\delta^{18}O$ records. See Table 2 and Methods for data sources and discussion of errors for all CO_2 and temperature estimates. Likely minimum global mean surface temperature is expressed relative to the pre-industrial (see Methods for details of calculation). The red and blue lines correspond to an ESS of 6 and 3 °C, respectively, as calculated from the 'max paleo-CO_2' line in panel A and a pre-industrial baseline of 280 ppm. The orange lines represent an ESS of 6 °C up to the point of ice sheet decay (assumed to be triggered at 560 ppm CO_2, or one doubling; DeConto & Pollard, 2003; Pollard & DeConto, 2005; Royer, 2006; DeConto *et al.*, 2008; Pearson *et al.*, 2009), then 3 °C thereafter in an ice-free world. The dashed lines represent an ESS of 3 °C and a constant 2000 ppm CO_2. All ESS reference lines account for solar evolution but not continental position. The blue band in panel B is the range of pre-industrial tropical SST (27–29 °C). (D) Calculation of ESS from the 'max paleo-CO_2' line in panel A and the benthic temperature data in panel C, after accounting for solar evolution and either including or excluding the impact of continental position (see Methods). These ESS estimates are likely underestimates (see Methods). Each data point is a 1 million-year mean; errors (±1σ) only take into account variance of the individual estimates. Time-steps represented by <5 data points are not shown. Dashed line is an ESS reference of 3 °C.

conditions. In contrast, our methodology returns a global temperature of 9.0–16.5 °C for the same tropical SST spread. This discrepancy reinforces our conservative approach in estimating ESS.

For benthic $\delta^{18}O$ temperature records, we assume an ice-free ocean $\delta^{18}O$ of −1.2‰. We also assume a 1:1 scaling between high-latitude sourced deep-water and global temperatures during non-glacial times (Hansen *et al.*, 2008). While changes in high-latitude surface-ocean temperature are generally amplified over the global surface *ocean*, the effect is compensated, at least in part, by amplified temperature change over *land* surfaces (e.g., Barron *et al.*, 1993; Sloan & Rea, 1995; Renssen *et al.*, 2004; Winguth *et al.*, 2010; Lunt *et al.*, 2011). This 1:1 scaling, however, is not well constrained (Hansen *et al.*, 2008). To cast benthic-derived global surface temperatures relative to the pre-industrial, we note that deep-water temperatures just prior to the onset of Antarctic glaciation approximately 34 Ma were approximately 6 °C warmer than the pre-industrial (Zachos *et al.*, 2008). Global surface temperature at this time was probably >6 °C warmer owing to the limit on deep-water temperatures by the freezing point during glacial periods. For example, a 2:3 scaling between deep-water and global temperatures is present during the Pleistocene (Hansen *et al.*, 2008). In the spirit of establishing minimum changes in global surface temperature, we assume here a 1:1 scaling for glacial times too.

We determine the number of CO_2 doublings relative to pre-industrial time from the 'max paleo-CO_2' line in Fig. 1A and a pre-industrial value of 280 ppm. CO_2 doublings are then converted to a projection of global mean surface temperature assuming a constant ESS value (colored lines in Fig. 1B,C). In this formulation, all temperature data plotting above a particular reference ESS line have an associated ESS that exceeds the reference value. We also compute ESS directly from the 'max paleo-CO_2' history and individual temperature estimates (1 million-year averages shown in Fig. 1D). Because CO_2 was probably lower than our 'max paleo-CO_2' reference, the ESS calculations are minima. However, CO_2 proxies, especially the stomatal proxy, lose precision at higher CO_2 levels (see weakly-to-unbounded estimates in Fig. 1A) (Royer *et al.*, 2001a; Beerling *et al.*, 2009b); these CO_2 estimates are likely minima. We express ESS in terms of temperature change per CO_2 doubling; division by 3.7 converts units to temperature change per W m^{-2}. Because changes in radiative forcing in our data set are mostly under two CO_2 doublings, this conversion is reasonable (Colman & McAvaney, 2009), even after accounting for changes in solar luminosity and continental position (described next).

Because the preceding analyses are normalized to pre-industrial conditions, it is necessary to consider the additional effects of solar luminosity, continental position (including orography), and biological evolution, which impact temperature independently of CO_2. We account for the increase in solar luminosity over time (Gough, 1981) assuming a 3.7 W m^{-2} forcing per doubled CO_2. Quantifying the impact of paleogeography on global temperatures is less certain. GCMs configured to the Cretaceous and early Paleogene, but with present-day luminosity, predict a warming of 0–2.8 °C relative to present-day control runs (Barron *et al.*, 1993; Sloan & Rea, 1995; Heinemann *et al.*, 2009; Dunkley Jones *et al.*, 2010); using the climate sensitivities of the individual models (Table 3), this effect is equivalent to 0–0.6 CO_2 doublings. A limitation of the results is that their associated models exclude ice sheets, making direct comparisons to the present-day difficult, unless changing geography alone is sufficient to melt all ice sheets. In this regard, the calculated warmings probably represent maxima. Bice *et al.* (2000) varied geography for a pair of simulations at 55 and 15 Ma (ice and greenhouse gas concentrations held constant) and found little difference in global temperature (0.6 °C, or 0.3 CO_2 doublings). Similarly, Donnadieu *et al.* (2006) performed simulations for the early and late Cretaceous and predicted a 3.8 °C warmer late Cretaceous (1.1 CO_2 doublings). Changes in vegetation as a result of continental configuration can also impact climate. Vegetation models dynamically coupled to climate models for the Cretaceous and Cenozoic predict a 1.9–2.2 °C warming (0.8–0.9 CO_2 doublings) over geographically equivalent simulations with either no vegetation or a present-day vegetation distribution (Dutton & Barron, 1997; Otto-Bliesner & Upchurch, 1997). Because the paleovegetation schemes were prescribed based on fossil evidence, which in turn reflect a combination of geographic, evolutionary, and greenhouse gas forcings, we consider these data to represent a maximum effect.

Table 3 Climate sensitivity (CS) of climate models used to evaluate the roles of continental position and vegetative feedbacks

Study	CS (°C)
Barron *et al.* (1993)	2.7
Sloan & Rea (1995)	2.1
Dutton & Barron (1997)	2.5*
Otto-Bliesner & Upchurch (1997)	2.5*
Bice *et al.* (2000)	2.5*
Donnadieu *et al.* (2006)	3.3†
Heinemann *et al.* (2009)	6.2
Dunkley Jones *et al.* (2010)	3.6

*CS not reported. Most other studies using the same family of models (NCAR GENESIS) for the Cretaceous and Paleogene report a CS between 2 and 3 °C (Barron *et al.*, 1993; Shellito *et al.*, 2003; Shellito *et al.*, 2009; Sloan & Rea, 1995).

†Y. Donnadieu, pers. comm., 2011.

We parameterize the impact of solar evolution and continental position on ESS as

$$\mathrm{ESS} = \frac{\Delta T(t)}{\log_2 \frac{CO_2(t)}{CO_2(0)} + \frac{\Delta S(t)}{3.7\,\mathrm{W\,m^{-2}}} + \frac{\Delta T_{geo}(t)}{CS}} \qquad (3)$$

where $\Delta T(t)$ and $\Delta S(t)$ are the global mean surface temperature (°C) and global mean solar irradiance (W m^{-2}), respec-

tively, at time t relative to pre-industrial conditions. Solar irradiance is determined by dividing the solar constant by four to account for the distribution of point-source radiation on a sphere and multiplying by 1-albedo, assumed here to be the present-day value of 0.7 for all time periods. $\Delta T_{geo}(t)$ is the component of $\Delta T(t)$ related to continental position and linked vegetation changes, and CS is the CS of the model used to calculate $\Delta T_{geo}(t)$ (Table 3). In the denominator of equation (3), the leftmost ratio is the number of CO_2 doublings at time t relative to pre-industrial conditions. The middle ratio is the radiative forcing of a younger sun expressed in CO_2 doublings; at 125 Ma, for example, the luminosity correction is −0.62 CO_2 doublings or −1.86 °C for the 3 °C ESS reference line (note overall positive slope of reference lines in Fig. 1B,C). The rightmost ratio is the effect of continental position and linked vegetation changes, also expressed in CO_2 doublings. Because $\Delta T_{geo}(t)$ is likely the least constrained term in equation (3), we calculate ESS two ways (see Fig. 1D): assuming no paleogeography effect ($\Delta T_{geo}(t) = 0$), and assuming a constant effect equivalent to one CO_2 doubling, which is near the upper bound of current constraints (see earlier discussion). The true value of $\Delta T_{geo}(t)$ probably lies between these bounds.

In summary, our formulation of ESS treats nearly all of the processes that impact temperature as part of the response to CO_2, not as external forcings. These include the dynamics of ice sheets, aerosols, clouds, and other GHGs. We therefore assume that these components vary as a function of climate state (see Discussion). Two variables that we treat as external forcings are solar evolution and continental position (and linked vegetation changes). Biological evolution also should be treated as a forcing independent of CO_2, but constraints are presently lacking. Two important evolutionary events since the Cretaceous that may have impacted CS via land surface albedo changes are the rise of angiosperms and grasslands.

Calculation of Earth system climate sensitivity: 65-0 Ma

The second ESS analysis focuses on the last 65 million years, which overlaps in time with the Cretaceous-early Paleogene analysis and includes a glaciated interval (last approximately 34 million years). The analysis follows many of the same principles already outlined. The key difference for the Cenozoic is that because data quality and quantity are generally high throughout, a more robust approach is possible. First, 1 million-year time-steps are computed from the mean benthic temperature curve of Hansen *et al.* (2008) (based on the compilation of Zachos *et al.*, 2008) and the mean CO_2 curve updated from Beerling & Royer (2011) (based on 391 individual CO_2 estimates; see Table 2 for sources). As already discussed, change in deep-sea temperature is a good minimum predictor of global surface temperature change: during glacial periods, surface temperature change is likely amplified over that of the deep sea, and during non-glacial times, the changes are similar within moderate uncertainty bounds. The radiative forcings of CO_2 change and solar evolution are combined (see previous section) and regressed directly against temperature change for the full time series to compute a single, average ESS. To place an upper constraint on the impact of continental position, we repeat the calculation assuming a paleogeography forcing equivalent to one CO_2 doubling for all Paleocene and Eocene data (see previous section; see also Micheels *et al.*, 2011 and Knorr *et al.*, 2011).

RESULTS

Cretaceous and early Paleogene

According to our new compilation of Cretaceous and early Paleogene proxy data, maximum atmospheric CO_2 declined from approximately 1000 ppm at 120 Ma to approximately 700 ppm at 58 Ma, followed by a spike to near 2000 ppm at 50 Ma (Figs 1A and 2A). Both global temperature reconstructions follow the same pattern (Fig. 1B,C), highlighting a first-order link between CO_2 and temperature. Both benthic and tropical SST approaches to estimating ESS are broadly complementary, with a large part of the Cretaceous and early Paleogene record yielding ESS estimates of 3 °C or higher. During the early Late Cretaceous (95-85 Ma), ESS may have exceeded 6 °C based on relatively poorly constrained CO_2 estimates (Fig. 1B,C).

We consider a minimum ESS of 3 °C for parts of the Cretaceous and Paleogene robust for several reasons. First, both the CO_2 and tropical SST records are internally consistent across methods, suggesting no strong methodological biases. However, because there are far fewer tropical data than benthic $\delta^{18}O$ data, we place more confidence in ESS estimates derived from deep-water temperature reconstructions (Fig. 1C,D). Second, given the uncertainties in the CO_2 proxies (Fig. 1A), estimates based on the 'max paleo-CO_2' line are potentially too low. However, even if we assume that CO_2 values were consistently high (2000 ppm), ESS would still exceed 3 °C for much of the interval (dotted lines in Fig. 1B,C). Third, because our results describe the mean ESS between the pre-industrial and a given geologic time slice, they could be biased by high ESS during glacial times (34-0 Ma). But even if glacial ESS was as high as 6 °C (Table 1), non-glacial ESS would still exceed 3 °C for some of the interval (orange lines in Fig. 1B,C). Fourth, although the impact of paleogeography is poorly constrained, ESS exceeds 3 °C for part of the interval, particularly during the Cretaceous, even if a strong paleogeographic effect is assumed (equivalent to one CO_2 doubling) (Fig. 1D).

Earth system climate sensitivity is not likely static over time, although given the uncertainties in the calculations a constant ESS cannot be excluded (Fig. 1D). This potential variability

impacts our calculations because they are based on comparing an ancient time slice to pre-industrial conditions. Thus, the calculations are buffered in the sense that they are biased toward the mean ESS between tie-points. We note that this effect does not undermine our general conclusion of >3 °C ESS, but it is nonetheless informative to explore higher resolution patterns. One way forward is to use two ancient tie-points and avoid the pre-industrial altogether. While such a calculation also returns a mean ESS, the tie-points are more closely spaced. An additional benefit to this approach is that it circumvents many of the potential problems with calculating global mean surface temperature (see Methods) because one paleotemperature is subtracted from another. Also, the potential confounding effects of geography and biological evolution are minimized. A drawback, however, is that problems related to uncertainties in the paleoclimate reconstructions tend to be magnified twofold. Thus, we consider the calculations provisional. If, in the future, uncertainties in the proxies are reduced and a clearer paleoclimatic picture emerges, the approach of calculating ESS from two closely spaced ancient tie-points would be superior to the approach adopted here (Fig. 1).

As noted earlier, the period from 58 to 50 Ma is marked by global warming (Fig. 1B,C). If we use the 'max paleo-CO_2' trajectory and an overall 5.5 °C rise in global temperature (5.75–11.25 °C from benthic records; 2.0–7.5 °C from Mg/Ca tropical SST records), ESS during this interval is 3.7 °C. For the period 100-58 Ma, with a ΔT of −3.75 °C from benthic records, the corresponding ESS is 6.4 °C.

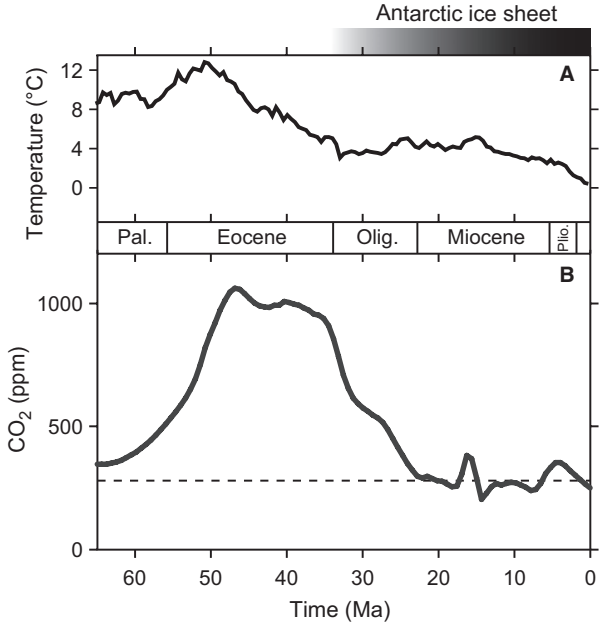

Fig. 2 Cenozoic CO_2 and temperature records. Temperature record is from Hansen *et al.* (2008), which is based on the benthic $\delta^{18}O$ record of Zachos *et al.* (2008), and is a rough minimum estimate of global surface temperature change relative to pre-industrial conditions (see Methods). CO_2 record is updated from Beerling & Royer (2011) (see Table 2 for original sources); dashed line is the pre-industrial value (280 ppm).

Cenozoic

The CO_2 and temperature histories for the last 65 million years (Fig. 2) have improved greatly in the last decade (Beerling & Royer, 2011), although important uncertainties still remain: CO_2 estimates for any given time slice vary up to about twofold (Beerling & Royer, 2011) and converting deep-sea temperature to global surface temperature is not straightforward (see Methods). As with the Cretaceous and early Paleogene analysis, the goal here is to provide some

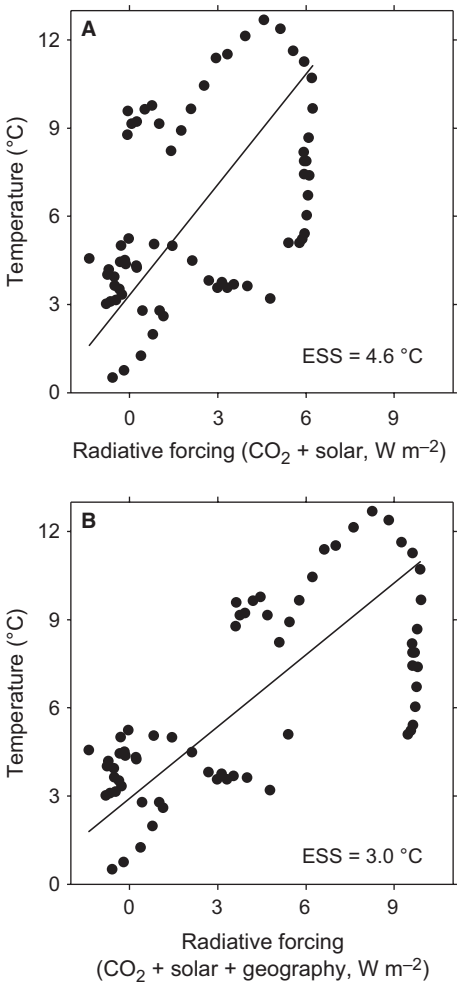

Fig. 3 Relationship between CO_2 radiative forcing and temperature for Cenozoic. Data points are 1 million-year time-steps of the data series in Fig. 2 and are expressed relative to pre-industrial conditions. (A) Calculation of Earth system sensitivity (ESS) taking into account solar evolution (see Methods). Slope of standardized major axis regression corresponds to an ESS of 4.6 °C per doubled CO_2, assuming 3.7 W m^{-2} per doubled CO_2. (B) Calculation of ESS taking into account solar evolution and assuming a radiative impact of continental position equivalent to one CO_2 doubling for all pre-Oligocene data (see Methods). Slope of regression corresponds to an ESS of 3.0 °C.

general constraints on ESS, not best-fit estimates. The primary difference for the Cenozoic is that there is sufficient data coverage to directly regress, at a higher temporal resolution (1 million-year time-steps), the full time series of temperature against the radiative forcing associated with doubled CO_2 and solar evolution. Following this approach, CO_2 and temperature are clearly linked (Fig. 3A; $r^2 = 0.20$; $P < 0.001$). The slope of the resulting regression, 1.25 °C per W m^{-2}, corresponds to an ESS of 4.6 °C. This calculation assumes no impact from continental position, which was probably less than the equivalent of one CO_2 doubling (see Methods). If an upper value of one CO_2 doubling is adopted for all pre-Oligocene data, the mean Cenozoic ESS drops to 3.0 °C (Fig. 3B; slope = 0.81 °C per W m^{-2}; $r^2 = 0.48$; $P < 0.001$).

With both analyses, there is considerable scatter about the regressions, likely reflecting both true variation in ESS and error in the paleoclimate data. Overall, our results strongly suggest that ESS probably exceeded 3 °C for part of the Cenozoic, even if the radiative impact of continental position was large. There are hints that ESS may have been higher during the glacial post-Eocene (cluster of data in lower-left corners of Fig. 3A,B), as would be expected, but presently the data fidelity are not high enough to conclude this with confidence.

DISCUSSION

Our provisional analyses indicate that ESS was at least 3 °C during some of the Cretaceous and Cenozoic. We stress that this 3 °C value is not a mean 'best-fit' estimate, but rather a likely minimum because many ESS estimates exceed 3 °C and because our methodology is designed to establish a minimum baseline (maximum CO_2 change, minimum temperature change). How do these ESS estimates compare to Charney sensitivity? In the present-day climate system, IPCC (2007) considers <1.5 °C very unlikely (<10% probability) and the most likely range (with 66% confidence) between 2.0 and 4.5 °C. However, a comparison to Charney sensitivity for the ancient past is more appropriate than that for the present-day. Critically, GCMs for the Cretaceous and early Eocene simulate a mean Charney sensitivity of 2.0–2.8 °C (Barron *et al.*, 1993; Sloan & Rea, 1995; Shellito *et al.*, 2003, 2009).

The totality of evidence suggests an ESS of at least 3 °C for part of the Cretaceous and Cenozoic (Figs 1B–D and 2) compared to a mean Charney sensitivity of 2.0–2.8 °C. We conclude from this that ESS was elevated relative to Charney sensitivity for at least some of the interval. Positive climate feedbacks probably existed during ice-free times that are either weak or absent today, or operate on timescales too long to be captured by most GCMs. This model-data mismatch has consequences for understanding Earth system dynamics during these warm periods, for example, the long-standing failure of GCMs in underestimating high-latitude temperatures and overestimating latitudinal temperature gradients (Barron *et al.*, 1993; Wing & Greenwood, 1993; Greenwood & Wing, 1995; Valdes, 2000, 2011; Shellito *et al.*, 2003, 2009; Schrag & Alley, 2004; Zachos *et al.*, 2008; Bijl *et al.*, 2009; Heinemann *et al.*, 2009; Huber & Caballero, 2011; Pope *et al.*, 2011).

What feedbacks are responsible for high ESS during non-glacial times?

The identity of these 'missing' feedbacks is uncertain. However, several biological feedbacks constitute 'known unknowns', including other GHGs and biogenic aerosols that could affect calculated ESS. Emissions of reactive biogenic gases from terrestrial ecosystems have substantial impacts on atmospheric chemistry (Arneth *et al.*, 2010). In particular, they influence the tropospheric concentrations of GHGs such as ozone, methane, and nitrous oxide. Polar ice core records indicate that the biogeochemical processes controlling atmospheric CH_4 and N_2O concentrations are sensitive to climate change on glacial-interglacial (Spahni *et al.*, 2005) and millennial timescales (Flückiger *et al.*, 2004). However, climate feedbacks of these trace GHGs are missing from most pre-Pleistocene climate modeling investigations that adopt fixed pre-industrial values, regardless of the prescribed atmospheric CO_2 concentration.

Methane is a radiatively important GHG, and wetlands are the largest natural source of methane to the atmosphere. Sedimentary evidence indicates that methane-producing wetland environments were more extensive in the past, particularly in the early Eocene, with the potential steady-state flux sufficient to raise atmospheric concentrations to several thousand parts per billion (Beerling *et al.*, 2009a). This, in turn, could also lead to higher stratospheric water vapor and polar stratospheric clouds (PSCs), because of oxidation, and result in surface warming. However, the associated uncertainty here is high because the very large changes in PSCs are prescribed rather than evolved in a self-consistent manner from the models (Sloan *et al.*, 1992; Kirk-Davidoff *et al.*, 2002). Three-dimensional 'earth system' modeling studies (latitude × longitude × height) characterizing ecosystem-chemistry climate interactions in the early Eocene (55 Ma) and late Cretaceous (90 Ma) greenhouse worlds independently indicate the potential for sustained elevated concentrations of methane (4–5× pre-industrial levels) and other trace GHGs at these times (Beerling *et al.*, 2011). Higher concentrations of trace GHGs exert a global planetary heating of approximately 2–3 °C amplified by lower surface albedo feedbacks in the high latitudes to >6 °C in the late Cretaceous and early Eocene (Beerling *et al.*, 2011). Experimental studies suggest elevated atmospheric CO_2 concentration can affect methane emissions from wetland systems (Megonigal & Schlesinger, 1997; Saarnio *et al.*, 2000; Ellis *et al.*, 2009). Hence, there should be feedback between atmospheric CO_2 and CH_4, which has strong relevance to understanding ESS. This expectation is supported by 3D earth system simulations showing a

similar CO_2 dependency of wetland CH_4 fluxes that increased ESS ($2 \times CO_2$ to $4 \times CO_2$) by 1–4 °C during the late Cretaceous and early Eocene (Beerling *et al.*, 2011).

Inclusion of ecosystem–atmospheric chemistry interactions into pre-Pleistocene GCMs highlights a further neglected biological feedback involving the effects of biogenic emissions of volatile organic compounds, which can partition into the solid phase to form secondary organic aerosols (SOA) (Carslaw *et al.*, 2010). SOA affect the radiative balance of the atmosphere directly by scattering incoming solar radiation and indirectly through the formation cloud condensation nuclei (CCN) (Carslaw *et al.*, 2010). The climate feedbacks of the ecosystem-aerosol interactions have yet to be investigated for the past or the present-day but could be important contributory factors influencing ESS (Arneth *et al.*, 2010). However, the atmospheric concentration of SOA is determined by emissions of volatile organic compounds from terrestrial ecosystems, and changes in temperature, humidity, precipitation, causing complex nonlinear interactions under warmer or cooler climate regimes. Current understanding suggests increased SOA loading in the future may represent a negative climate feedback (Carslaw *et al.*, 2010) that could decrease ESS to a CO_2 doubling.

In terms of marine biogenic aerosols, Kump & Pollard (2008) obtained dramatic results from prescribed reductions in marine aerosol production by phytoplankton in the Cretaceous. Assuming thermal stress in the Cretaceous oceans reduced dimethlysulfide production by phytoplankton, these idealized calculations led to a reduced abundance of CCN and less extensive cloud cover. Whether such assumptions are justified for past glacial and non-glacial climate states remains to be investigated. Nevertheless, as a result of decreased cloud cover reducing the reflection of incoming solar energy, polar temperatures rose dramatically by 10–15 °C (Kump & Pollard, 2008). Clearly, the properties of aerosols leading to cloud formation are an important and neglected aspect of GCM assessment of ESS both for present-day and past climates. This issue is highlighted by recent work suggesting that cloud parameterization schemes in climate models may be tuned to a modern 'dirty' atmosphere, giving an unrepresentatively high abundance of CCN compared to that expected in a pristine pre-industrial atmosphere (Kiehl, 2009). More appropriate constraints on CCN could therefore exert profound effects on climate simulations of continental interiors of past warm climate intervals (Kiehl, 2009). Unfortunately, our level of scientific understanding for all of these 'known unknowns' is very low. This necessarily limits confidence in ESS estimates derived from the current generation of GCMs.

CONCLUSIONS

A growing body of evidence supports an ESS often exceeding 6 °C during glacial times and 3 °C during non-glacial times. These estimates are likely higher than the abundant estimates of CS that include only a subset of fast feedbacks most appropriate for the present-day Earth system (Charney CS, approximately 3 °C). The feedbacks responsible for the disparity in a non-glaciated world are not well known because they are (presumably) weak-to-absent today and thus difficult to identify with Earth observation programs. Nonetheless, geological evidence and GCMs implicate clouds and other trace GHGs as possible candidates. As these missing feedbacks are clarified, they can be incorporated into standard runs of paleo-GCMs to address long-standing model-data mismatches, particularly the estimation by models of too-cool high latitudes. More robust GCMs will not only improve our understanding of climate dynamics in ancient greenhouse times, but also improve future climate predictions as we move toward a new greenhouse world.

ACKNOWLEDGMENTS

We thank Matthew Huber, Dorian Abbot, Rodrigo Caballero, Ken Caldeira, Jerry Dickens, and David Archer for helpful comments on the manuscript, and Yannick Donnadieu for data access. D. L. R. thanks the Mellon Foundation for supporting a College of the Environment fellowship. M. P. acknowledges support from National Science Foundation and the Yale Climate and Energy Institute. D. J. B. gratefully acknowledges support through a Royal Society-Wolfson Research Merit Award.

REFERENCES

Archer D (2005) Fate of fossil fuel CO_2 in geologic time. *Journal of Geophysical Research* **110**, C09S05.

Archer D, Brovkin V (2008) The millennial atmospheric lifetime of anthropogenic CO_2. *Climatic Change* **90**, 283–297.

Armour KC, Roe GH (2011) Climate commitment in an uncertain world. *Geophysical Research Letters* **38**, L01707.

Arneth A, Harrison SP, Zaehle S, Tsigaridis K, Menon S, Bartlein PJ, Feichter J (2010) Terrestrial biogeochemical feedbacks in the climate system. *Nature Geoscience* **3**, 525–532.

Barron EJ, Fawcett PJ, Pollard D, Thompson S (1993) Model simulations of Cretaceous climates: the role of geography and carbon dioxide. *Philosophical Transactions of the Royal Society London B* **341**, 307–316.

Beerling DJ, Royer DL (2011) Convergent Cenozoic CO_2 history. *Nature Geoscience* **4**, 418–420.

Beerling DJ, Lomax BH, Royer DL, Upchurch GR, Kump LR (2002) An atmospheric pCO_2 reconstruction across the Cretaceous-Tertiary boundary from leaf megafossils. *Proceedings of the National Academy of Sciences of the USA* **99**, 7836–7840.

Beerling D, Berner RA, Mackenzie FT, Harfoot MB, Pyle JA (2009a) Methane and the CH_4-related greenhouse effect over the past 400 million years. *American Journal of Science* **309**, 97–113.

Beerling DJ, Fox A, Anderson CW (2009b) Quantitative uncertainty analyses of ancient atmospheric CO_2 estimates from fossil leaves. *American Journal of Science* **309**, 775–787.

Beerling DJ, Fox A, Stevenson DS, Valdes PJ (2011) Enhanced chemistry-climate feedbacks in past greenhouse worlds. *Proceedings of the National Academy of Sciences of the USA* **108**, 9770–9775.

Bice KL, Norris RD (2002) Possible atmospheric CO_2 extremes of the Middle Cretaceous (late Albian-Turonian). *Paleoceanography* **17**, 1070.

Bice KL, Scotese CR, Seidov D, Barron EJ (2000) Quantifying the role of geographic change in Cenozoic ocean heat transport using uncoupled atmosphere and ocean models. *Palaeogeography Palaeoclimatology Palaeoecology* **161**, 295–310.

Bice KL, Birgel D, Metyers PA, Dahl KA, Hinrichs K-U, Norris RD (2006) A multiple proxy and model study of Cretaceous upper ocean temperatures and atmospheric CO_2 concentration. *Paleoceanography* **21**, PA2002.

Bijl PK, Schouten S, Sluijs A, Reichart G-J, Zachos JC, Brinkhuis H (2009) Early Palaeogene temperature evolution of the southwest Pacific Ocean. *Nature* **461**, 776–779.

Bijl PK, Houben AJP, Schouten S, Bohaty SM, Sluijs A, Reichart G-J, Sinninghe Damsté JS, Brinkhuis H (2010) Transient Middle Eocene atmospheric CO_2 and temperature variations. *Science* **330**, 819–821.

Bornemann A, Norris RD, Friedrich O, Beckmann B, Schouten S, Sinninghe Damsté JS, Vogel J, Hofmann P, Wagner T (2008) Isotopic evidence for glaciation during the Cretaceous supergreenhouse. *Science* **319**, 189–192.

Borzenkova II (2003) Determination of global climate sensitivity to the gas composition of the atmosphere from paleoclimatic data. *Izvestiya, Atmospheric and Oceanic Physics* **39**, 197–202.

Breecker DO, Sharp ZD, McFadden LD (2009) Seasonal bias in the formation and stable isotopic composition of pedogenic carbonate in modern soils from central New Mexico, USA. *Geological Society of America Bulletin* **121**, 630–640.

Breecker DO, Sharp ZD, McFadden LD (2010) Atmospheric CO_2 concentrations during ancient greenhouse climates were similar to those predicted for A.D. 2100. *Proceedings of the National Academy of Sciences of the USA* **107**, 576–580.

Brierley CM, Fedorov AV (2010) Relative importance of meridional and zonal sea surface temperature gradients for the onset of the ice ages and Pliocene-Pleistocene climate evolution. *Paleoceanography* **25**, PA2214.

Budyko MI, Ronov AB, Yanshin AL (1987) *History of the Earth's Atmosphere*, Springer-Verlag, Berlin.

van der Burgh J, Visscher H, Dilcher DL, Kürschner WM (1993) Paleoatmospheric signatures in Neogene fossil leaves. *Science* **260**, 1788–1790.

Carslaw KS, Boucher O, Spracklen DV, Mann GW, Rae JGL, Woodward S, Kulmala M (2010) A review of natural aerosol interactions and feedbacks within the Earth system. *Atmospheric Chemistry and Physics* **10**, 1701–1737.

Charney JG, Arakawa A, Baker DJ, Bolin B, Dickinson RE, Goody RM, Leith CE, Stommel HM, Wunsch CI (1979) *Carbon Dioxide and Climate: a Scientific Assessment.* National Academy of Sciences Press, Washington, DC.

Chen JL, Wilson CR, Tapley BD (2006) Satellite gravity measurements confirm accelerated melting of Greenland ice sheet. *Science* **313**, 1958–1960.

Colman R, McAvaney B (2009) Climate feedbacks under a very broad range of forcing. *Geophysical Research Letters* **36**, L01702.

Covey C, Sloan LC, Hoffert MI (1996) Paleoclimate data constraints on climate sensitivity: the paleocalibration method. *Climatic Change* **32**, 165–184.

Cramer BS, Toggweiler JR, Wright JD, Katz ME, Miller KG (2009) Ocean overturning since the Late Cretaceous: inferences from a new benthic foraminiferal isotope compilation. *Paleoceanography* **24**, PA4216.

Crowley TJ, Zachos JC (2000) Comparison of zonal temperature profiles for past warm time periods. In *Warm Climates in Earth History* (eds Huber BT, MacLeod KG, Wing SL). Cambridge University Press, Cambridge, pp. 50–76.

DeConto RM, Pollard D (2003) Rapid Cenozoic glaciation of Antarctica induced by declining atmospheric CO_2. *Nature* **421**, 245–249.

DeConto RM, Pollard D, Wilson PA, Pälike H, Lear CH, Pagani M (2008) Thresholds for Cenozoic bipolar glaciation. *Nature* **455**, 652–656.

Donnadieu Y, Pierrehumbert R, Jacob R, Fluteau F (2006) Modelling the primary control of paleogeography on Cretaceous climate. *Earth and Planetary Science Letters* **248**, 426–437.

Doria G, Royer DL, Wolfe AP, Fox A, Westgate JA, Beerling DJ (2011) Declining atmospheric CO_2 during the late Middle Eocene climate transition. *American Journal of Science* **311**, 63–75.

Dumitrescu M, Brassell SC, Schouten S, Hopmans EC, Sinninghe Damsté JS (2006) Instability in tropical Pacific sea-surface temperatures during the early Aptian. *Geology* **34**, 833–836.

Dunkley Jones T, Ridgwell A, Lunt DJ, Maslin MA, Schmidt DN, Valdes PJ (2010) A Paleogene perspective on climate sensitivity and methane hydrate instability. *Philosophical Transactions of the Royal Society London A* **368**, 2395–2415.

Dutton JE, Barron EJ (1997) Miocene to present vegetation changes: a possible piece of the Cenozoic cooling puzzle. *Geology* **25**, 39–41.

Ellis T, Hill PW, Fenner N, Williams GG, Godbold D, Freeman C (2009) The interactive effects of elevated carbon dioxide and water table draw-down on carbon cycling in a Welsh ombrotrophic bog. *Ecological Engineering* **35**, 978–986.

Fletcher BJ, Brentnall SJ, Anderson CW, Berner RA, Beerling DJ (2008) Atmospheric carbon dioxide linked with Mesozoic and early Cenozoic climate change. *Nature Geoscience* **1**, 43–48.

Flückiger J, Blunier T, Stauffer B, Chappellaz J, Spahni R, Kawamura K, Schwander J, Stocker TF, Dahl-Jensen D (2004) N_2O and CH_4 variations during the last glacial epoch: insight into global processes. *Global Biogeochemical Cycles* **18**, GB1020.

Forster A, Schouten S, Baas M, Sinninghe Damsté JS (2007a) Mid-Cretaceous (Albian Santonian) sea surface temperature record of the tropical Atlantic Ocean. *Geology* **35**, 919–922.

Forster A, Schouten S, Moriya K, Wilson PA, Sinninghe Damsté JS (2007b) Tropical warming and intermittent cooling during the Cenomanian/Turonian oceanic anoxic event 2: sea surface temperature records from the equatorial Atlantic. *Paleoceanography* **22**, PA1219.

Frakes LA, Francis JE, Syktus JI (1992) *Climate Modes of the Phanerozoic.* Cambridge University Press, Cambridge.

Friedlingstein P, Solomon S, Plattner GK, Knutti R, Ciais P, Raupach MR (2011) Long-term climate implications of twenty-first century options for carbon dioxide emission mitigation. *Nature Climate Change* **1**, 457–461.

Gillett NP, Arora VK, Zickfeld K, Marshall SJ, Merryfield WJ (2011) Ongoing climate change following a complete cessation of carbon dioxide emissions. *Nature Geoscience* **4**, 83–87.

Gough DO (1981) Solar interior structure and luminosity variations. *Solar Physics* **74**, 21–34.

Greenwood DR, Wing SL (1995) Eocene continental climates and latitudinal temperature gradients. *Geology* **23**, 1044–1048.

Greenwood DR, Scarr MJ, Christophel DC (2003) Leaf stomatal frequency in the Australian tropical rainforest tree *Neolitsea dealbata* (Lauraceae) as a proxy measure of atmospheric pCO_2. *Palaeogeography Palaeoclimatology Palaeoecology* **196**, 375–393.

Hansen J, Sato M, Kharecha P, Beerling D, Berner R, Masson-Delmotte V, Pagani M, Raymo M, Royer DL, Zachos JC (2008) Target atmospheric CO_2: where should humanity aim? *Open Atmospheric Science Journal* **2**, 217–231.

Haworth M, Hesselbo SP, McElwain JC, Robinson SA, Brunt JW (2005) Mid-Cretaceous pCO_2 based on stomata of the extinct conifer *Pseudofrenelopsis* (Cheirolepidiaceae). *Geology* **33**, 749–752.

Heinemann M, Jungclaus JH, Marotzke J (2009) Warm Paleocene/Eocene climate as simulated in ECHAM5/MPI-OM. *Climate of the Past* **5**, 785–802.

Higgins JA, Schrag DP (2006) Beyond methane: towards a theory for the Paleocene-Eocene Thermal Maximum. *Earth and Planetary Science Letters* **245**, 523–537.

Hoffert MI, Covey C (1992) Deriving global climate sensitivity from palaeoclimate reconstructions. *Nature* **360**, 573–576.

Hollis CJ, Handley L, Crouch EM, Morgans HEG, Baker JA, Creech J, Collins KS, Gibbs SJ, Huber M, Schouten S, Zachos JC, Pancost RD (2009) Tropical sea temperatures in the high-latitude South Pacific during the Eocene. *Geology* **37**, 99–102.

Huber M (2008) A hotter greenhouse? *Science* **321**, 353–354.

Huber M, Caballero R (2011) The early Eocene equable climate problem revisited. *Climate of the Past* **7**, 603–633.

IPCC (2007) *Climate Change 2007: The Physical Science Basis, Contribution of Working Group I to the Fourth Assessment Report of the Intergovernmental Panel on Climate Change* (eds Solomon S, Qin D, Manning M, Chen Z, Marquis M, Averyt KB, Tignor M, Miller HL). Cambridge University Press, Cambridge, pp. 996.

Jagniecki E, Lowenstein TK, Jenkins D (2010) Sodium carbonates: temperature and pCO_2 indicators for ancient and modern alkaline saline lakes. *Geological Society of America Abstracts with Programs* **42**, 404 (Paper No. 165-402).

Kiehl JT (2009) Challenges in modeling warm Cenozoic climates. *Geochimica et Cosmochimica Acta* **73**(S1), A648.

Kiehl JT (2011) Lessons from Earth's past. *Science* **331**, 158–159.

Kim J-H, Schouten S, Hopmans EC, Donner B, Sinninghe Damsté JS (2008) Global sediment core-top calibration of the TEX_{86} paleothermometer in the ocean. *Geochimica et Cosmochimica Acta* **72**, 1154–1173.

Kirk-Davidoff DB, Schrag DP, Anderson JG (2002) On the feedback of stratospheric clouds and polar climate. *Geophysical Research Letters* **29**, doi: 10.1029/2002GL014659.

Klochko K, Kaufman AJ, Yao WS, Byrne RH, Tossell JA (2006) Experimental measurement of boron isotope fractionation in seawater. *Earth and Planetary Science Letters* **248**, 276–285.

Klochko K, Cody GD, Tossell JA, Dera P, Kaufman AJ (2009) Re-evaluating boron speciation in biogenic calcite and aragonite using ^{11}B MAS NMR. *Geochimica et Cosmochimica Acta* **73**, 1890–1900.

Knorr G, Butzin M, Micheels A, Lohmann G (2011) A warm Miocene climate at low atmospheric CO_2 levels. *Geophysical Research Letters* **38**, L20701.

Knutti R, Hegerl GC (2008) The equilibrium sensitivity of the Earth's temperature to radiation changes. *Nature Geoscience* **1**, 735–743.

Kump LR, Pollard D (2008) Amplification of Cretaceous warmth by biological cloud feedbacks. *Science* **320**, 195.

Kürschner WM, van der Burgh J, Visscher H, Dilcher DL (1996) Oak leaves as biosensors of late Neogene and early Pleistocene paleoatmospheric CO_2 concentrations. *Marine Micropaleontology* **27**, 299–312.

Kürschner WM, Wagner F, Dilcher DL, Visscher H (2001) Using fossil leaves for the reconstruction of Cenozoic paleoatmospheric CO_2 concentrations. In *Geological Perspectives of Global Climate Change* (eds Gerhard LC, Harrison WE, Hanson BM). The American Association of Petroleum Geologists, Tulsa, OK, pp. 169–189.

Kürschner WM, Kvacek Z, Dilcher DL (2008) The impact of Miocene atmospheric carbon dioxide fluctuations on climate and the evolution of terrestrial ecosystems. *Proceedings of the National Academy of Sciences of the USA* **105**, 449–453.

Lemarchand D, Gaillardet J, Lewin É, Allègre CJ (2000) The influence of rivers on marine boron isotopes and implications for reconstructing past ocean pH. *Nature* **408**, 951–954.

Lloyd AH (2005) Ecological histories from Alaskan tree lines provide insight into future change. *Ecology* **86**, 1687–1695.

Lowenstein TK, Demicco RV (2006) Elevated Eocene atmospheric CO_2 and its subsequent decline. *Science* **313**, 1928.

Lunt DJ, Haywood AM, Schmidt GA, Salzmann U, Valdes PJ, Dowsett HJ (2010) Earth system sensitivity inferred from Pliocene modelling and data. *Nature Geoscience* **3**, 60–64.

Lunt DJ, Valdes PJ, Dunkley Jones T, Ridgwell A, Haywood AM, Schmidt DN, Marsh R, Maslin M (2011) CO_2-driven ocean circulation changes as an amplifier of Paleocene-Eocene thermal maximum hydrate destablilization. *Geology* **38**, 875–878.

Matthews HD, Caldeira K (2008) Stabilizing climate requires near-zero emissions. *Geophysical Research Letters* **35**, L04705.

McElwain JC (1998) Do fossil plants signal palaeoatmospheric CO_2 concentration in the geological past? *Philosophical Transactions of the Royal Society London B* **353**, 83–96.

Megonigal JP, Schlesinger WH (1997) Enhanced CH_4 emission from a wetland soil exposed to elevated CO_2. *Biogeochemistry* **37**, 77–88.

Micheels A, Bruch AA, Eronen J, Fortelius M, Harzhauser M, Utescher T, Mosbrugger V (2011) Analysis of heat transport mechanisms from a Late Miocene model experiment with a fully-coupled atmosphere–ocean general circulation model. *Palaeogeography Palaeoclimatology Palaeoecology* **304**, 337–350.

Montenegro A, Brovkin V, Eby M, Archer D, Weaver AJ (2007) Long term fate of anthropogenic carbon. *Geophysical Research Letters* **34**, L19707.

Moriya K, Wilson PA, Friedrich O, Erbacher J, Kawahata H (2007) Testing for ice sheets during the mid-Cretaceous greenhouse using glassy foraminiferal calcite from the mid-Cenomanian tropics on Demerara Rise. *Geology* **35**, 615–618.

Norris RD, Bice KL, Magno EA, Wilson PA (2002) Jiggling the tropical thermostat in the Cretaceous hothouse. *Geology* **30**, 299–302.

Otto-Bliesner BL, Upchurch GR (1997) Vegetation-induced warming of high-latitude regions during the Late Cretaceous period. *Nature* **385**, 804–807.

Pagani M, Lemarchand D, Spivack A, Gaillardet J (2005a) A critical evaluation of the boron isotope-*p*H proxy: the accuracy of ancient ocean *p*H estimates. *Geochimica et Cosmochimica Acta* **69**, 953–961.

Pagani M, Zachos JC, Freeman KH, Tipple B, Bohaty S (2005b) Marked decline in atmospheric carbon dioxide concentrations during the Paleogene. *Science* **309**, 600–603.

Pagani M, Caldeira K, Archer D, Zachos JC (2006) An ancient carbon mystery. *Science* **314**, 1556–1557.

Pagani M, Liu Z, LaRiviere J, Ravelo AC (2010) High Earth-system climate sensitivity determined from Pliocene carbon dioxide concentrations. *Nature Geoscience* **3**, 27–30.

Pagani M, Huber M, Liu Z, Bohaty SM, Henderiks J, Sijp W, Krishnan S, Deconto RM (2011) The role of carbon dioxide during the onset of Antarctic glaciation. *Science* **334**, 1261–1264.

Park J, Royer DL (2011) Geologic constraints on the glacial amplification of Phanerozoic climate sensitivity. *American Journal of Science* **311**, 1–26.

Passalia MG (2009) Cretaceous pCO_2 estimation from stomatal frequency analysis of gymnosperm leaves of Patagonia, Argentina. *Palaeogeography Palaeoclimatology Palaeoecology* **273**, 17–24.
Pearson PN, Palmer MR (2000) Atmospheric carbon dioxide concentrations over the past 60 million years. *Nature* **406**, 695–699.
Pearson PN, Ditchfield PW, Singano J, Harcourt-Brown KG, Nicholas CJ, Olsson RK, Shackleton NJ, Hall MA (2001) Warm tropical sea surface temperatures in the Late Cretaceous and Eocene epochs. *Nature* **413**, 481–487.
Pearson PN, van Dongen BE, Nicholas CJ, Pancost RD, Schouten S, Singano JM, Wade BS (2007) Stable warm tropical climate through the Eocene Epoch. *Geology* **35**, 211–214.
Pearson PN, McMillan IK, Wade BS, Jones TD, Coxall HK, Bown PR, Lear CH (2008) Extinction and environmental change across the Eocene-Oligocene boundary in Tanzania. *Geology* **36**, 179–182.
Pearson PN, Foster GL, Wade BS (2009) Atmospheric carbon dioxide through the Eocene-Oligocene climate transition. *Nature* **461**, 1110–1113.
Pollard D, DeConto RM (2005) Hysteresis in Cenozoic Antarctic ice-sheet variations. *Global and Planetary Change* **45**, 9–21.
Pope JO, Collins M, Haywood AM, Dowsett HJ, Hunter SJ, Lunt DJ, Pickering SJ, Pound MJ (2011) Quantifying uncertainty in model predictions for the Pliocene (Plio-QUMP): initial results. *Palaeogeography Palaeoclimatology Palaeoecology* **309**, 128–140.
Pucéat E, Lécuyer C, Donnadieu Y, Naveau P, Cappetta H, Ramstein G, Huber BT, Kriwet J (2007) Fish tooth $\delta^{18}O$ revising Late Cretaceous meridional upper ocean water temperature gradients. *Geology* **35**, 107–110.
Quan C, Sun G, Zhou Z (2010) A new Tertiary *Ginkgo* (Ginkgoaceae) from the Wuyun formation of Jiayin, Heilongjiang, northeastern China and its paleoenvironmental implications. *American Journal of Botany* **97**, 446–457.
Raymo ME, Grant B, Horowitz M, Rau GH (1996) Mid-Pliocene warmth: stronger greenhouse and stronger conveyor. *Marine Micropaleontology* **27**, 313–326.
Renssen H, Beets CJ, Fichefet T, Goosse H, Kroon D (2004) Modeling the climate response to a massive methane release from gas hydrates. *Paleoceanography* **19**, PA2010.
Retallack GJ (2009) Greenhouse crises of the past 300 million years. *Geological Society of America Bulletin* **121**, 1441–1455.
Roe GH, Armour KC (2011) How sensitive is climate sensitivity? *Geophysical Research Letters* **38**, L14708.
Roe GH, Baker MB (2007) Why is climate sensitivity so unpredictable? *Science* **318**, 629–632.
Royer DL(2003) Estimating latest Cretaceous and Tertiary atmospheric CO_2 concentration from stomatal indices. In *Causes and Consequences of Globally Warm Climates in the Early Paleogene* (eds Wing SL, Gingerich PD, Schmitz B, Thomas E). Geological Society of America Special Paper 369, Boulder, CO, pp. 79–93.
Royer DL (2006) CO_2-forced climate thresholds during the Phanerozoic. *Geochimica et Cosmochimica Acta* **70**, 5665–5675.
Royer DL (2010) Fossil soils constrain ancient climate sensitivity. *Proceedings of the National Academy of Sciences of the USA* **107**, 517–518.
Royer DL, Berner RA, Beerling DJ (2001a) Phanerozoic CO_2 change: evaluating geochemical and paleobiological approaches. *Earth-Science Reviews* **54**, 349–392.
Royer DL, Wing SL, Beerling DJ, Jolley DW, Koch PL, Hickey LJ, Berner RA (2001b) Paleobotanical evidence for near present-day levels of atmospheric CO_2 during part of the Tertiary. *Science* **292**, 2310–2313.
Royer DL, Berner RA, Park J (2007) Climate sensitivity constrained by CO_2 concentrations over the past 420 million years. *Nature* **446**, 530–532.
Rustad JR, Zarzycki P (2008) Calculation of site-specific carbon-isotope fractionation in pedogenic oxide minerals. *Proceedings of the National Academy of Sciences of the USA* **105**, 10297–10301.
Saarnio S, Saarinen T, Vasander H, Silvola J (2000) A moderate increase in the annual CH_4 efflux by raised CO_2 or NH_4NO_3 supply in a boreal oligotrophic mire. *Global Change Biology* **6**, 137–144.
Schouten S, Hopmans EC, Forster A, van Breugel Y, Kuypers MMM, Sinninghe Damsté JS (2003) Extremely high sea-surface temperatures at low latitudes during the middle Cretaceous as revealed by archaeal membrane lipids. *Geology* **31**, 1069–1072.
Schrag DP, Alley RB (2004) Ancient lessons for our future climate. *Science* **306**, 821–822.
Seki O, Foster GL, Schmidt DN, Mackensen A, Kawamura K, Pancost RD (2010) Alkenone and boron-based Pliocene *p*CO2 records. *Earth and Planetary Science Letters* **292**, 201–211.
Sexton PF, Wilson PA, Pearson PN (2006) Microstructural and geochemical perspectives on planktic foraminiferal preservation: ''glassy'' versus ''frosty''. *Geochemistry Geophysics Geosystems* **7**, Q12P19.
Shaffer G, Olsen SM, Pedersen JOP (2009) Long-term ocean oxygen depletion in response to carbon dioxide emissions from fossil fuels. *Nature Geoscience* **2**, 105–109.
Shellito CJ, Sloan LC, Huber M (2003) Climate model sensitivity to atmospheric CO_2 levels in the Early-Middle Paleogene. *Palaeogeography Palaeoclimatology Palaeoecology* **193**, 113–123.
Shellito CJ, Lamarque J-F, Sloan LC (2009) Early Eocene Arctic climate sensitivity to pCO_2 and basin geography. *Geophysical Research Letters* **36**, L09707.
Sloan LC, Rea DK (1995) Atmospheric carbon dioxide and early Eocene climate: a general circulation modeling sensitivity study. *Palaeogeography Palaeoclimatology Palaeoecology* **119**, 275–292.
Sloan LC, Walker JCG, Moore TC, Rea DK, Zachos JC (1992) Possible methane-induced polar warming in the early Eocene. *Nature* **357**, 320–322.
Smith RY, Greenwood DR, Basinger JF (2010) Estimating paleoatmospheric pCO_2 during the Early Eocene Climatic Optimum from stomatal frequency of *Ginkgo*, Okanagan Highlands, British Columbia, Canada. *Palaeogeography Palaeoclimatology Palaeoecology* **293**, 120–131.
Soden BJ, Held IM (2006) An assessment of climate feedbacks in coupled ocean-atmosphere models. *Journal of Climate* **19**, 3354–3360.
Solomon S, Plattner G-K, Knutti R, Friedlingstein P (2009) Irreversible climate change due to carbon dioxide emissions. *Proceedings of the National Academy of Sciences of the USA* **106**, 1704–1709.
Solomon S, Daniel JS, Sanford TJ, Murphy DM, Plattner G-K, Knutti R, Friedlingstein P (2010) Persistence of climate changes due to a range of greenhouse gases. *Proceedings of the National Academy of Sciences of the USA* **107**, 18354–18359.
Spahni R, Chappellaz J, Stocker TF, Loulergue L, Hausammann G, Kawamura K, Flückiger J, Schwander J, Raynaud D, Masson-Delmotte V, Jouzel J (2005) Atmospheric methane and nitrous oxide of the Late Pleistocene from Antarctic ice cores. *Science* **310**, 1317–1321.
Sturm M, Racine C, Tape K (2001) Increasing shrub abundance in the Arctic. *Nature* **411**, 546–547.
Tipple BJ, Meyers SR, Pagani M (2010) Carbon isotope ratio of Cenozoic CO_2: a comparative evaluation of available geochemical proxies. *Paleoceanography* **25**, PA3202.
Tripati A, Delaney ML, Zachos JC, Anderson LD, Kelly DC, Elderfield H (2003) Tropical sea-surface temperature reconstruction for

the early Paleogene using Mg/Ca ratios of planktonic foraminifera. *Paleoceanography* **18**, 1101.

Tripati AK, Roberts CD, Eagle RA (2009) Coupling of CO_2 and ice sheet stability over major climate transitions of the last 20 million years. *Science* **326**, 1394–1397.

Valdes PJ (2000) Warm climate forcing mechanisms. In *Warm Climates in Earth History* (eds Huber BT, MacLeod KG, Wing SL). Cambridge University Press, Cambridge, pp. 3–20.

Valdes PJ (2011) Built for stability. *Nature Geoscience* **4**, 414–416.

Vaughan APM (2007) Climate and geology – a Phanerozoic perspective. In *Deep-Time Perspectives on Climate Change: Marrying the Signal from Computer Models and Biological Proxies* (eds Williams M, Haywood AM, Gregory FJ, Schmidt DN). The Geological Society and the Micropalaeontological Society, Special Publications, London, pp. 5–59.

Wagner T, Herrle JO, Sinninghe Damsté JS, Schouten S, Stüsser I, Hofmann P (2008) Rapid warming and salinity changes of Cretaceous surface waters in the subtropical North Atlantic. *Geology* **36**, 203–206.

Wilson PA, Norris RD (2001) Warm tropical ocean surface and global anoxia during the mid-Cretaceous period. *Nature* **412**, 425–429.

Wilson PA, Opdyke BN (1996) Equatorial sea-surface temperatures for the Maastrichtian revealed through remarkable preservation of metastable carbonate. *Geology* **24**, 555–558.

Wilson PA, Norris RD, Cooper MJ (2002) Testing the Cretaceous greenhouse hypothesis using glassy foraminiferal calcite from the core of the Turonian tropics on Demerara Rise. *Geology* **30**, 607–610.

Wing SL, Greenwood DR (1993) Fossils and fossil climate: the case for equable continental interiors in the Eocene. *Philosophical Transactions of the Royal Society London B* **341**, 243–252.

Winguth A, Shellito C, Shields C, Winguth C (2010) Climate response at the Paleocene-Eocene thermal maximum to greenhouse gas forcing – a model study with CCSM3. *Journal of Climate* **23**, 2563–2584.

Zachos J, Pagani M, Sloan L, Thomas E, Billups K (2001) Trends, rhythms, and aberrations in global climate 65 Ma to present. *Science* **292**, 686–693.

Zachos JC, Dickens GR, Zeebe RE (2008) An early Cenozoic perspective on greenhouse warming and carbon-cycle dynamics. *Nature* **451**, 279–283.

Zeebe RE, Zachos JC, Dickens GR (2009) Carbon dioxide forcing alone insufficient to explain Palaeocene-Eocene Thermal Maximum warming. *Nature Geoscience* **2**, 576–580.